THEORY OF RADIATIVE $\boldsymbol{B}$ DECAYS*

Mikołaj Misiak

Institute of Theoretical Physics, Warsaw University
Hoża 69, 00-681 Warsaw, Poland
e-mail: `Mikolaj.Misiak@fuw.edu.pl`

(Received May 7, 2001)

The status of theoretical calculations of $\mathrm{BR}[\bar{B} \to X_s\gamma]$ is discussed. It is pointed out that replacing $m_c^{\rm pole}/m_b^{\rm pole}$ in the matrix element $\langle X_s\gamma|(\bar{s}c)_{V-A}(\bar{c}b)_{V-A}|b\rangle$ by the more appropriate $m_c^{\overline{\rm MS}}(\mu)/m_b^{\rm pole}$ with $\mu \in [m_c, m_b]$ causes an 11% enhancement of the SM prediction for the branching ratio, and has a sizeable effect on the uncertainty. However, the uncertainty can be maintained at the level of around 10% thanks to an observation that $m_b(\mu)$ in the top-quark contribution to the decay amplitude is the main source of perturbative QCD effects in the considered process.

PACS numbers: 13.20.He

The purpose of the present paper is discussing the status of theoretical calculations of the inclusive branching ratio $\mathrm{BR}_\gamma \equiv \mathrm{BR}[\bar{B} \to X_s\gamma]$ in the SM. Many elements our considerations are directly applicable also to other weak radiative $\bar{B}$ decays to charmless particles, in particular to the exclusive modes $\bar{B} \to K^*\gamma$ and $\bar{B} \to \rho\gamma$, as well as to the inclusive decay $\bar{B} \to X_d\gamma$.

The leading electroweak transitions that mediate $\bar{B} \to X_s\gamma$ are shown in Fig. 1. The dominant contribution originates from charm-quark loops. The top-quark contribution is more than twice smaller (after resumming QCD logarithms) and comes with an opposite sign. The u-quark diagrams are CKM-suppressed, and play a minor role.

Since the charm contribution is dominant, the existing determinations of $|V_{ts}|$ from BR_γ heavily rely on the unitarity of 3×3 CKM matrix. On the other hand, the very unitarity implies that $|V_{ts}|$ is very close in size to $|V_{cb}|$.

* Presented at the Cracow Epiphany Conference on b Physics and CP Violation, Cracow, Poland, January 5–7, 2001.

The latter quantity is well determined from the semileptonic $\bar{B}$ decays. Thus, BR_γ can hardly improve our knowledge of the Wolfenstein parameters or provide us with accurate tests of CKM unitarity.

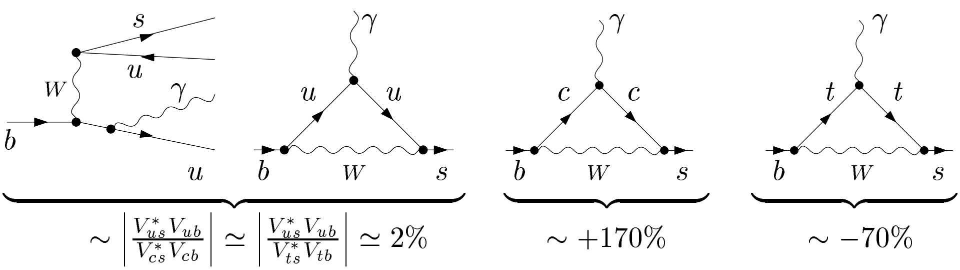

Fig. 1. Examples of leading-order electroweak diagrams for $\bar{B} \to X_s\gamma$.

However, BR_γ is well known as a good testing ground for extensions of the SM. The reasons for this are as follows:

- The decay $\bar{B} \to X_s\gamma$ arises mainly at one loop in the SM. Moreover, its SM branching ratio turns out to be quite small when compared to naive expectations. Therefore, its sensitivity to electroweak-scale exotica is particularly large.
- All the parameters that are relevant for the SM prediction are well measured in other processes.
- There is no overall non-perturbative factor in the theoretical expression for the decay amplitude, contrary *e.g.* to the $B\bar{B}$ and $K\bar{K}$ mixing or to $\bar{B}_s \to \mu^+\mu^-$ that require lattice inputs at present. In $\bar{B} \to X_s\gamma$ (within certain range of photon energy cut-offs), non-perturbative effects enter only as corrections, in analogy to the inclusive semileptonic decay $\bar{B} \to X_c e\bar{\nu}_e$.
- The $\bar{B} \to X_s\gamma$ amplitude in the SM is suppressed by $m_b/M_W \ll 1$. This suppression can be relaxed in certain popular extensions of the SM (*e.g.* in the MSSM with large $\tan\beta$ [1–3] or in the left–right symmetric models [4–6]). Then, the sensitivity of BR_γ to exotic particles goes much above the electroweak scale (up to $\Lambda \sim M_W^2/m_b \simeq 1.3$ TeV), even if the CKM matrix remains the only source of flavour violation.

Of course, the power of BR_γ for testing new physics crucially depends on how accurate its measurements are and how accurate the theoretical prediction is. The current experimental results are as follows:

$$\mathrm{BR}[\bar{B}\to X_s\gamma] = (2.85 \pm 0.35_{\mathrm{stat.}} \pm 0.22_{\mathrm{syst.}}) \times 10^{-4} \qquad \text{(CLEO [7])},$$
$$\mathrm{BR}[\bar{B}\to X_s\gamma] = \left[3.37 \pm 0.53_{\mathrm{stat.}} \pm 0.42_{\mathrm{syst.}} \left({}^{+0.50}_{-0.54}\right)_{\mathrm{model}}\right]\times 10^{-4} \qquad \text{(Belle [8])},$$
$$\mathrm{BR}[b\to s\gamma] = (3.11 \pm 0.80_{\mathrm{stat.}} \pm 0.72_{\mathrm{syst.}})\times 10^{-4} \qquad \text{(ALEPH [9])}.$$

The weighted average for BR_γ is therefore[1]

$$\mathrm{BR}_\gamma^{\mathrm{exp}} = (2.96 \pm 0.35) \times 10^{-4}, \tag{1}$$

with an error of around 12%. New results from CLEO, Belle and BaBar are expected soon. However, our limited knowledge of the photon energy spectrum may restrict the accuracy of comparing theory with experiment.

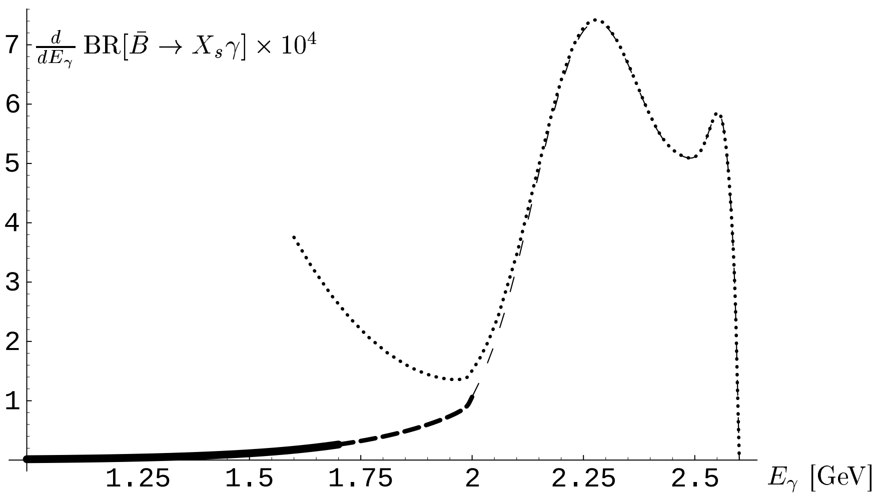

Fig. 2. An "artist view" of $\frac{d}{dE_\gamma}\mathrm{BR}[\bar{B} \to X_s\gamma]$.

The $\bar{B} \to X_s\gamma$ photon spectrum in the $\bar{B}$-meson rest frame is shown in Fig. 2. The solid and dashed lines describe the spectrum without the intermediate ψ contribution (*i.e.* the contribution from $\bar{B} \to X_s\psi$ followed by $\psi \to X'\gamma$). The dotted line shows how the spectrum changes when the intermediate ψ contribution is included[2]. This contribution has been effectively treated as background in all the existing analyses of $\bar{B} \to X_s\gamma$, both on the experimental and theoretical sides. This convention will be followed below.

[1] Statistical errors in the ALEPH measurement of $b \to s\gamma$ are much larger than expected differences among weak radiative branching ratios of the included b-hadrons.

[2] It is a very rough estimate, based on the measured spectra of $\bar{B} \to X\psi$ [10] and (boosted) $\psi \to X'\gamma$ [11].

The thickness of the solid and dashed lines in Fig. 2 reflects the degree of confidence with which the shape of the spectrum is theoretically known. The prediction is quite solid where the line is solid. For higher energies, it is only an “artist view” how the spectrum could look like. We know that there is a peak, and we can determine the size of this peak, because the total inclusive decay rate is calculable [12] within the Heavy Quark Effective Theory (HQET)[3]. However, the shape of the peak can be determined only experimentally. In this respect, the recent results of CLEO [7] are very interesting. Unfortunately, their present energy cut-off $E_\gamma > 2$ GeV is still quite high[4]. Consequently, the present comparison of theory and experiment must rely on a model-dependent extrapolation of the photon energy spectrum [13, 14]. Hopefully, this issue might become less problematic once the photon energy spectrum above the cut-off is more precisely measured.

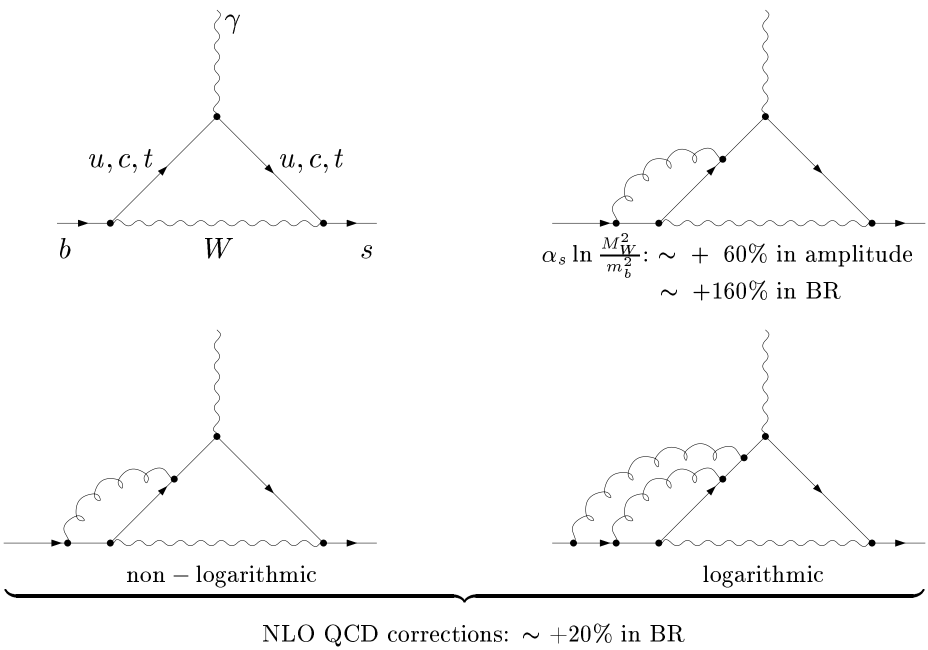

Fig. 3. Examples of Feynman diagrams contributing to $b \to s\gamma$ at various orders in the renormalization-group improved perturbation theory.

[3] A few moments of the photon spectrum are calculable, too.

[4] Moreover, it is imposed in the LAB frame rather than in the $\bar{B}$-meson rest frame. The photon energies in the two frames can differ by as much as ±135 MeV.

Below, in the discussion of theoretical results for BR_γ, we shall assume that the photon energy cut-off is already low enough, *e.g.* $E_\gamma > 1.6$ GeV in the $\bar{B}$-meson rest frame. In such a case, the dominant contribution to BR_γ is given by the partonic decay $b \to X_s\gamma$ of the b-quark.

Examples of diagrams that contribute to the perturbative $b \to s\gamma$ amplitude are shown in Fig. 3. The leading one-loop diagrams were calculated twenty years ago [15]. Seven years later, it was realized [16, 17] that logarithmic two-loop QCD effects are very large. An enhancement of BR_γ by a factor of 2.6 (for $m_t = 175$ GeV) was found after resummation of $\left(\alpha_s \ln M_W^2/m_b^2\right)^n$ to all orders in n with the help of renormalization-group techniques [18–24].

Since the perturbative uncertainties at the Leading Order (LO) were large [25], a calculation of the Next-to-Leading-Order (NLO) QCD corrections to $b \to s\gamma$ was undertaken (see the second row in Fig. 3). It required calculating logarithmic parts of two- and three-loop diagrams [26, 27] as well as non-logarithmic parts of two-loop diagrams, including their low-momentum [28] and high-momentum [29–33] regions. The corresponding bremsstrahlung corrections were evaluated earlier [34, 35]. Large QCD logarithms were resummed in all those analyses.

The calculated NLO QCD corrections enhance BR_γ by another 20%. The electroweak [13, 36–38] and non-perturbative [39–44] corrections have smaller effects. The overall uncertainty in the prediction for BR_γ is still dominated by perturbative QCD. It was estimated in Refs. [13, 27, 45, 46]. However, only the latter paper properly accounts for errors due to m_c/m_b. In consequence, the predicted value of BR_γ is significantly higher than in the previous analyses. The uncertainty can be maintained at the level of around 10% thanks to an observation that $m_b(\mu)$ in the top-quark contribution to the decay amplitude is the main source of QCD effects. In the remainder of this paper, we shall discuss those very recent developments.

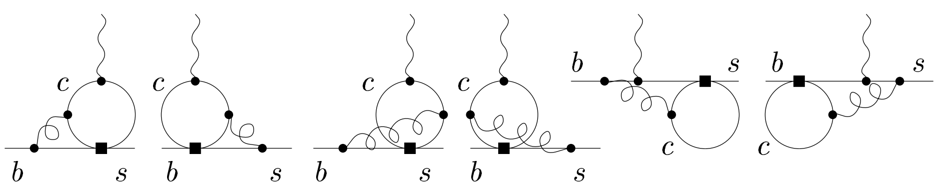

Fig. 4. Leading contributions to the matrix element $\langle s\gamma|(\bar{s}c)_{V-A}(\bar{c}b)_{V-A}|b\rangle$.

The (m_c/m_b) dependence of the $b \to s\gamma$ amplitude arises from two-loop diagrams with charm quarks calculated by Greub, Hurth and Wyler [28]. Such 1PI diagrams are shown in Fig. 4. The W-boson propagator has been contracted to a point, so those diagrams represent a matrix element of the four-quark operator $(\bar{s}c)_{V-A}(\bar{c}b)_{V-A}$. Since the dependence of such a matrix element on m_c/m_b is quite strong, we should ask what renormalization scheme should be used for quark masses. Should we use $m_c^{\rm pole}/m_b^{\rm pole} = 0.29 \pm 0.02$ or, perhaps, $m_c^{\overline{\rm MS}}(\mu)/m_b^{\rm pole} \approx 0.22 \pm 0.04$ (with $\mu \in [m_c, m_b]$)? In principle, such a question is a NNLO issue, *i.e.* it is as relevant as three-loop corrections to the diagrams in Fig. 4. However, it is numerically very important, because changing m_c/m_b from 0.29 to 0.22 in the considered matrix element implies an increase of BR_γ by 11%, *i.e.* by as much as the present experimental and theoretical uncertainties.

Since calculating three-loop corrections to the diagrams in Fig. 4 would be a very difficult task at present, we have to guess what the optimal choice of m_c and m_b is, on the basis of our experience from other calculations. All the factors of m_c in the considered diagrams originate from explicit mass factors in the charm-quark propagators. In the real part of the considered amplitude, those charm quarks are dominantly off-shell, with momentum scale μ set by m_b. Actually, we are not able to decide whether this scale is m_b, $\frac{1}{2}m_b$ or $\frac{1}{3}m_b$. Therefore, it seems reasonable to vary μ between $m_c \sim \frac{1}{3}m_b$ and m_b, and use $m_c^{\overline{\rm MS}}(\mu)$ in the ratio m_c/m_b.

As far as the factors of m_b in the considered diagrams are concerned, they originate either from the overall momentum release in $b \to s\gamma$ or from the explicit appearance of m_b in the b-quark propagators. In the first case, the appropriate choice of m_b is a low-virtuality mass. In the second case, there is no intuitive argument that could tell us whether $m_b^{\rm pole}$ or $m_b(m_b)$ is preferred. However, so long as the three-loop diagrams remain unknown, setting all the

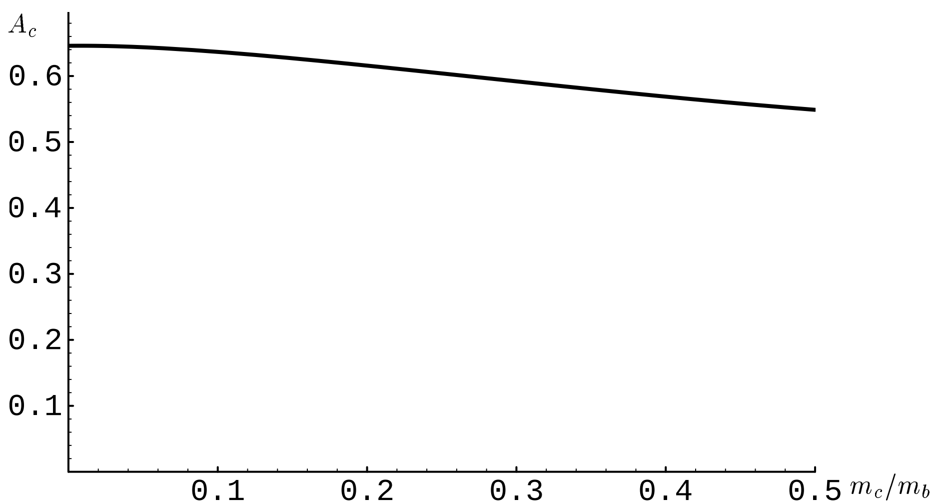

Fig. 5. Charm-loop contribution to the NLO amplitude of $b \to s\gamma$ as a function of m_c/m_b .

factors of m_b equal to $m_b^{\rm pole}$ seems to be a good choice. Even a better choice is the so-called $1S$-mass of the b-quark [47,48] that is defined as half of the perturbative contribution to the Υ mass. It is leading-renormalon free and differs from $m_b^{\rm pole}$ only by 1% at one loop.

The LO contribution to BR_γ is independent of m_c. Only the NLO corrections are m_c dependent. Thus, it seems surprising at the first glance that a change of m_c/m_b from 0.29 to 0.22 causes an increase of BR_γ by as much as 11%. Fig. 5 presents the charm-loop contribution A_c to the NLO amplitude of $b \to s\gamma$ (in arbitrary units) as a function of m_c/m_b. One can see that the dependence of A_c on the quark mass ratio is not extremely strong at all. When m_c/m_b changes from 0 to $\frac{1}{2}$, A_c decreases by around 16%, *i.e.* the NLO correction to A_c changes from plus a few percent to minus a few percent. Such a change is not particularly big for a $\mathcal{O}(\alpha_s(m_b))$ correction. However, the negative interference with the top-loop contribution (see Fig. 1) implies that the full $b \to s\gamma$ amplitude changes by 25%, and BR_γ changes by 53%. Thus, a large effect in BR_γ can be caused by a relatively mild effect in A_c.

Once $m_c^{\overline{\rm MS}}(\mu)/m_b^{\rm pole}$ with $\mu \in [m_c, m_b]$ is used in Fig. 4, the uncertainty in BR_γ significantly increases. This is due in part to a strong scale-dependence of $m_c(\mu)$. Moreover, in all the previous analyses, the m_c dependence of $\Gamma[b \to s\gamma]$ canceled partially against that of the semileptonic decay rate that is conventionally used for normalization. Once the different nature of the charm mass in the two cases is appreciated, the cancellation no longer takes place.

Fortunately, it is possible to make several improvements in the calculation, which allows us to maintain the theoretical uncertainty at the level of around $\sim 10\%$. In particular, good control over the behaviour of QCD perturbation series in $\bar{B} \to X_s\gamma$ is achieved by splitting the charm- and top-quark-loop contributions to the decay amplitude. The overall factor of m_b is frozen at the electroweak scale in the top contribution to the effective vertex $m_b(\bar{s}_{\rm L}\sigma^{\mu\nu}b_{\rm R})F_{\mu\nu}$. All the remaining factors of m_b are expressed in terms of the bottom $1S$-mass. As argued in Ref. [47], expressing the kinematical factors of m_b in inclusive B-meson decay rates in terms of the $1S$-mass improves the behaviour of QCD perturbation series with respect to what would be obtained using $m_b^{\overline{\rm MS}}(m_b)$ or $m_b^{\rm pole}$. When such an approach is used, no sizeable accidental cancellations of scale-dependence in the NLO expressions for BR_γ are observed.

Splitting the charm and top contributions to the amplitude allows us to better understand the origin of the well-known factor of ~ 3 enhancement of BR_γ by QCD logarithms. When the splitting is performed at LO, the charm contribution is found to be extremely stable under QCD renormalization group evolution. The logarithmic enhancement of the branching ratio appears to be almost entirely due to the top-quark sector. It can be attributed to the large anomalous dimension of the b-quark mass.

In order to explain those issues in more detail, it is necessary to introduce the effective Lagrangian that is always used in $\bar{B} \to X_s \gamma$ analyses. It reads

$$\mathcal{L} = \mathcal{L}_{\mathrm{QCD}\times\mathrm{QED}}\,(u,d,s,c,b) + \frac{4G_{\mathrm{F}}}{\sqrt{2}} V_{ts}^* V_{tb} \sum_{i=1}^{8} C_i(\mu) P_i\,. \tag{2}$$

The first term above is just the QCD×QED Lagrangian for the light quarks, and the second term contains flavour-changing local interactions P_i of either 4 quarks or 2 quarks and gauge bosons.

$$P_i = \begin{cases} (\bar{s}\Gamma_i c)(\bar{c}\Gamma'_{\underline{i}} b), & i = 1,2, & |C_i(\mu_b)| \sim 1, \\ (\bar{s}\Gamma_i b)\sum_q (\bar{q}\Gamma'_{\underline{i}} q), & i = 3,4,5,6, & |C_i(\mu_b)| < 0.07, \\ \frac{e m_b}{16\pi^2} \bar{s}_{\mathrm{L}} \sigma^{\mu\nu} b_{\mathrm{R}} F_{\mu\nu}, & i = 7, & |C_7(\mu_b)| \sim 0.3, \\ \frac{g m_b}{16\pi^2} \bar{s}_{\mathrm{L}} \sigma^{\mu\nu} T^a b_{\mathrm{R}} G^a_{\mu\nu}, & i = 8, & |C_8(\mu_b)| \sim 0.15. \end{cases} \tag{3}$$

The symbols Γ_i and Γ'_i in P_1,..., P_6 stand for various products of the Dirac and colour matrices.

The resummation of large QCD logarithms in B decays usually begins with decoupling the heavy electroweak bosons and the top-quark. In the resulting effective theory (2), flavour-changing interactions are present only in operators P_i (3). Their Wilson coefficients $C_i(\mu)$ evolve according to the Renormalization Group Equations (RGEs) from the matching scale $\mu_0 \sim (M_W \text{ or } m_t)$ down to the scale $\mu_b \sim m_b$ where the matrix elements of P_i are evaluated.

In the leading logarithmic approximation, the $b \to s\gamma$ amplitude is proportional to the (effective) Wilson coefficient of the operator P_7. The well-known [25] expression for this coefficient reads

$$C_7^{(0)\mathrm{eff}}(\mu_b) = \eta^{\frac{16}{23}} C_7^{(0)}(\mu_0) + \frac{8}{3}\left(\eta^{\frac{14}{23}} - \eta^{\frac{16}{23}}\right) C_8^{(0)}(\mu_0) + \sum_{i=1}^{8} h_i \eta^{a_i}, \tag{4}$$

where $\eta = \alpha_s(\mu_0)/\alpha_s(\mu_b)$ and

$$h_i = \left(\tfrac{626126}{272277} \;\; -\tfrac{56281}{51730} \;\; -\tfrac{3}{7} \;\; -\tfrac{1}{14} \;\; -0.6494 \;\; -0.0380 \;\; -0.0185 \;\; -0.0057 \right), \tag{5}$$

$$a_i = \left(\tfrac{14}{23} \;\; \tfrac{16}{23} \;\; \tfrac{6}{23} \;\; -\tfrac{12}{23} \;\; 0.4086 \;\; -0.4230 \;\; -0.8994 \;\; 0.1456 \right). \tag{6}$$

The coefficients $C_7^{(0)}(\mu_0)$ and $C_8^{(0)}(\mu_0)$ are found from the one-loop electroweak diagrams presented in Fig. 6. It is sufficient to calculate the 1PI diagrams only.

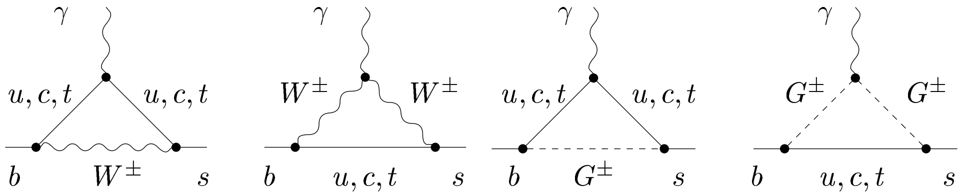

Fig. 6. One-loop 1PI diagrams for $b \to s\gamma$ in the SM.

Contributions from different internal quark flavours in those diagrams can be separately matched onto gauge-invariant operators, even when the calculation is performed off-shell[5]. For the operator P_7 and its gluonic analogue P_8, each quark flavour yields a UV-finite contribution that depends neither on the renormalization scheme nor on the gauge-fixing parameter.

When such a separation of flavours is made, and the CKM-suppressed u-quark contribution is neglected, Eq. (4) can be written as

$$C_7^{(0)\mathrm{eff}}(\mu_b) = X_c + X_t\,, \tag{7}$$

where the charm-quark contribution is given by

$$X_c \;=\; -\frac{23}{36}\eta^{\frac{16}{23}} - \frac{8}{9}\left(\eta^{\frac{14}{23}} - \eta^{\frac{16}{23}}\right) + \sum_{i=1}^{8} h_i \eta^{a_i}\,, \tag{8}$$

and the top-quark one reads

$$X_t \;=\; -\frac{1}{2}A_0^t\left(\frac{m_t^2}{M_W^2}\right)\eta^{\frac{16}{23}} - \frac{4}{3}F_0^t\left(\frac{m_t^2}{M_W^2}\right)\left(\eta^{\frac{14}{23}} - \eta^{\frac{16}{23}}\right), \tag{9}$$

where

$$\begin{aligned} A_0^t(x) &= \tfrac{-3x^3+2x^2}{2(x-1)^4}\ln x + \tfrac{-22x^3+153x^2-159x+46}{36(x-1)^3}\,, \\ F_0^t(x) &= \tfrac{3x^2}{2(x-1)^4}\ln x + \tfrac{-5x^3+9x^2-30x+8}{12(x-1)^3}\,. \end{aligned} \tag{10}$$

The first two terms in X_c (8) are obtained from Eq. (4) by the following replacements: $C_7^{(0)}(\mu_0) \to -\frac{23}{36}$ and $C_8^{(0)}(\mu_0) \to -\frac{1}{3}$, which is equivalent to including only charm contributions to the matching conditions for the corresponding operators. Analogously, only top loops contribute to X_t. The last term in Eq. (4) now appears in X_c, because it is entirely due to effects of

[5] In an off-shell calculation, use of the background-field gauge is necessary to ensure the absence of gauge-non-invariant operators. There is no $W^\pm G^\mp\gamma$ coupling in the background-field gauge.

charm loops in the RGE evolution. The splitting of charm and top is performed at the level of SM Feynman diagrams, and the effective theory is nothing but a technical tool for resumming large QCD logarithms in gluonic corrections to those diagrams.

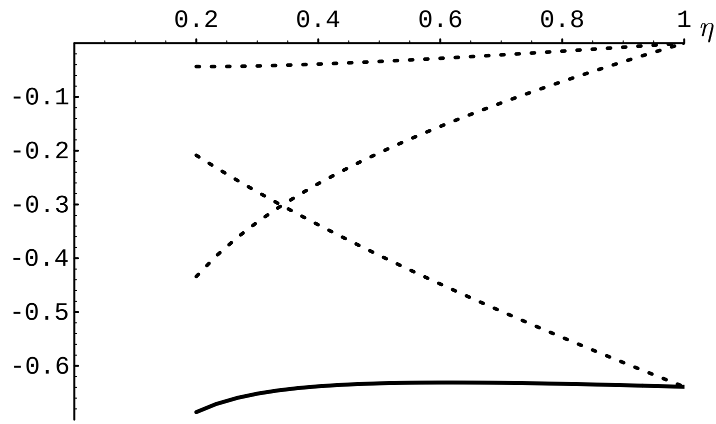

Fig. 7. X_c as a function of η (solid line), and its three components in Eq. (8) (dashed lines).

X_c is a function of η that varies very slowly in the physically interesting region $0.4 < \eta < 1$. This is illustrated in Fig. 7, where the three components of X_c in Eq. (8) are plotted as well. The second component is numerically small, while there is a strong cancellation of the η dependence between the first and the third component. However, these components are not separately physical in any conceivable limit, so the cancellation cannot be considered accidental.

Since X_c is practically scale-independent, X_t must be the source of the factor of $\sim$3 enhancement of BR_γ by QCD logarithms. This is indeed the case, because all the powers of η in Eq. (9) are positive and quite large. When η changes from unity to 0.566 (which corresponds to $\mu_0 = M_W$ and $\mu_b = 5$ GeV), then X_t decreases from 0.450 to 0.325. At the same time, X_c changes by only 0.008 (from $-\frac{23}{36} \approx -0.639$ to -0.631). Consequently, $|C_7^{(0)\mathrm{eff}}(\mu)|^2$ increases from 0.036 to 0.094, *i.e.* the branching ratio gets enhanced by a factor of 2.6.

It is easy to identify the reason for the strong η dependence of X_t. It is the large anomalous dimension of $m_b(\mu)$ that stands in front of the operator P_7 (3). The anomalous dimension γ_m is responsible for $\frac{12}{23}$ out of $\frac{16}{23}$ in the power of η that multiplies the (numerically dominant) function $A_0^t(x)$ in the expression for X_t.

Thus, the logarithmic QCD effects in $b \to s\gamma$ can be approximately taken into account by simply keeping m_b renormalized at $\mu_0 \sim (m_t \text{ or } M_W)$ in the top contribution to the decay amplitude. Motivated by this observation, we shall now rewrite the known NLO expressions for $\bar{B} \to X_s\gamma$ in such a manner. As we shall see, this simple operation not only allows us to reproduce the logarithmic QCD enhancement, but also the NLO corrections become significantly smaller than in the traditional approach. Moreover, the residual renormalization-scale-dependence diminishes, without any accidental cancellations involved. In other words, the behaviour of QCD perturbation series improves.

Our input here are the standard NLO QCD formulae for $B \to X_s\gamma$ collected in Ref. [27], and the separate charm-sector and top-sector matching conditions for the relevant operators presented in section 2 of Ref. [6]. Apart from the perturbative QCD effects, we shall include the electroweak and the available non-perturbative corrections. Assuming that the dominant NNLO QCD effects have the same origin as the dominant LO and NLO ones, we shall use all the currently known perturbative information to determine the ratio of $m_b(\mu_0)$ to the bottom $1S$-mass that normalizes the semileptonic decay rate.

The $\bar{B} \to X_s\gamma$ branching ratio with an energy cut-off E_0 in the $\bar{B}$-meson rest frame can be expressed as follows:

$$\mathrm{BR}[\bar{B} \to X_s\gamma]^{\text{subtracted } \psi,\, \psi'}_{E_\gamma > E_0}$$

$$= \mathrm{BR}[\bar{B} \to X_c e\bar{\nu}]_{\text{exp}} \left| \frac{V_{ts}^* V_{tb}}{V_{cb}} \right|^2 \frac{6\alpha_{\text{em}}}{\pi\, C} \left[P(E_0) + N(E_0) \right], \tag{11}$$

where $\alpha_{\text{em}} = \alpha_{\text{em}}^{\text{on shell}}$ [36] and $P(E_0)$ is given by the perturbative ratio

$$\frac{\Gamma[b \to X_s\gamma]_{E_\gamma > E_0}}{|V_{cb}/V_{ub}|^2\ \Gamma[b \to X_u e\bar{\nu}]} = \left| \frac{V_{ts}^* V_{tb}}{V_{cb}} \right|^2 \frac{6\alpha_{\text{em}}}{\pi}\ P(E_0)\,. \tag{12}$$

$N(E_0)$ denotes the non-perturbative correction[6]. Contrary to the standard approach, we have chosen the *charmless* semileptonic rate (corrected for the appropriate CKM angles) to be the normalization factor in Eq. (12). This modification is offset by the factor C in Eq. (11):

$$C = \left| \frac{V_{ub}}{V_{cb}} \right|^2 \frac{\Gamma[\bar{B} \to X_c e\bar{\nu}]}{\Gamma[\bar{B} \to X_u e\bar{\nu}]}\,. \tag{13}$$

[6] This means that $P(E_0)$ gets replaced by $P(E_0) + N(E_0)$ when b is replaced by $\bar{B}$ in Eq. (12).

This observable can either be measured or calculated. Our normalization to the *charmless* semileptonic rate in the l.h.s. of Eq. (12) is motivated by the need for separating the problem of m_c determination from the problem of convergence of perturbation series in $b \to X_s\gamma$. The factor C can be called "the non-perturbative semileptonic phase-space factor".

The perturbative quantity $P(E_0)$ can be written in the following form:

$$P(E_0) = \left| K_c + \left(1 + \frac{\alpha_s(\mu_0)}{\pi} \ln \frac{\mu_0^2}{m_t^2}\right) r(\mu_0) K_t + \varepsilon_{\rm ew} \right|^2 + B(E_0)\,, \qquad (14)$$

where K_t contains the top contributions to the $b \to s\gamma$ amplitude. K_c contains the remaining contributions, among which the charm loops are by far dominant. The electroweak correction to the $b \to s\gamma$ amplitude is denoted by $\varepsilon_{\rm ew}$. The ratio

$$r(\mu_0) = \frac{m_b^{\overline{\rm MS}}(\mu_0)}{m_b^{1S}} \qquad (15)$$

appears in Eq. (14) because we keep m_b renormalized at μ_0 in the top contribution to the operator P_7 (3), while all the kinematical factors of m_b are expressed in terms of the bottom $1S$-mass.

The bremsstrahlung function $B(E_0)$ contains the effects of $b \to s\gamma g$ and $b \to s\gamma q\bar{q}$ $(q = u, d, s)$ transitions. It is the only E_0 dependent part in $P(E_0)$. Its influence on the $b \to X_s\gamma$ branching ratio is less than 4% when 1 GeV $< E_0 <$ 2 GeV.

TABLE I

Numerical results.

	"naive"	LO	NLO
$\mathrm{Re}\, K_c$ $(\mu_0 = M_W)$	-0.639	-0.631 ± 0.003	-0.611 ± 0.002
$\mathrm{Re}\, K_t$ $(\mu_0 = m_t)$	0.450	0.434 ± 0.005	0.397 ± 0.003
$\mathrm{BR}_{E_\gamma > 1.6\,\mathrm{GeV}} \times 10^4$	3.53	3.56 ± 0.14	3.60 ± 0.05

In Table I, the numerical results are presented at various orders of the renormalization-group-improved perturbation theory. In the "naive" approach, the difference of $r(\mu_0)$ (15) from unity is the only included QCD effect. At LO, all the QCD logarithms $\left(\alpha_s \ln M_W^2/m_b^2\right)^n$ are taken into account. At NLO, we add the non-logarithmic $\mathcal{O}(\alpha_s)$ corrections, together with the electroweak and non-perturbative ones. The indicated errors correspond to varying the low-energy scale μ_b between $m_b/2$ and $2m_b$.

One can see that the behaviour of the QCD perturbation series for all the considered quantities is good, and that their residual μ_b dependence is quite weak. Such a weak μ_b dependence is not caused by any accidental cancellations. This is contrary to what was observed in many previous calculations. In the present approach, there is no indication that the unknown

NNLO corrections[7] could be much larger than $(\alpha_s(m_b)/\pi)^2 \approx 0.5\%$ times a factor of order unity. Consequently, our estimate of the overall uncertainty in the final prediction for BR_γ is not larger than in the previous analyses, despite taking the problems with m_c/m_b into account here.

When all the errors are included and added in quadrature, one finds

$$\mathrm{BR}[\bar{B} \to X_s\gamma]^{\text{subtracted } \psi,\, \psi'}_{E_\gamma > 1.6 \text{ GeV}} \;=\; (3.60 \pm 0.30) \times 10^{-4}. \tag{16}$$

In view of the fact that many of the published results have been calculated for $E_0 = m_b/20 \approx 0.23$ GeV (*i.e.* $\delta \equiv 1 - 2E_0/m_b = 0.9$), it is interesting to check what Eq. (11) gives in such a case. We find

$$\mathrm{BR}[\bar{B} \to X_s\gamma]_{E_\gamma > m_b/20} \;=\; (3.73 \pm 0.31) \times 10^{-4}. \tag{17}$$

It is the above result that should be compared [13] with the experimental weighted average (1) for the "total" branching ratio. The difference between theory and experiment is at the level of $1.6\,\sigma$. However, one should remember that the theoretical errors have no statistical interpretation, which implies that the value of $1.6\,\sigma$ has only an illustrative character.

If we used $m_c/m_b = 0.29$ instead of 0.22 in K_c and $B(E_0)$, we would find 3.35×10^{-4} for the branching ratio. The latter result is very close to the ones obtained in many previous analyses (see *e.g.* [13,38]). Thus, the replacement of $m_c^{\text{pole}}/m_b^{\text{pole}}$ by $m_c(\mu)/m_b^{1S}$ in $\langle s\gamma|(\bar{s}c)_{V-A}(\bar{c}b)_{V-A}|b\rangle$ is the main reason why our result is significantly higher than the previously published ones.

To conclude:

- An $\sim 11\%$ increase in the SM prediction for BR_γ is found when $m_c^{\text{pole}}/m_b^{\text{pole}}$ is replaced by the (more appropriate) $m_c(\mu)/m_b^{\text{pole}}$ in the NLO correction to the $b \to s\gamma$ amplitude.

- The well-known (factor of ~ 3) enhancement of BR_γ by leading QCD logarithms is mainly due to the evolution of m_b in the top-quark contribution to the amplitude.

- Including an explicit factor of $m_b(\mu_0)/m_b^{1S}$ in the NLO expressions allows us to control the residual scale-dependence more efficiently.

- The present prediction for the "total" branching ratio is

  $$\mathrm{BR}[\bar{B} \to X_s\gamma]_{E_\gamma > m_b/20} = (3.73 \pm 0.31) \times 10^{-4}, \tag{18}$$

  which differs by $1.6\,\sigma$ from the experimental world average

  $$\mathrm{BR}[\bar{B} \to X_s\gamma]_{\text{exp}} = (2.96 \pm 0.35) \times 10^{-4}. \tag{19}$$

[7] Except for those related to the ratio m_c/m_b that has been discussed above.

This research has been supported in part by the Polish State Committee for Scientific Research under grant 2 P03B 121 20, 2001-2003.

REFERENCES

[1] S. Bertolini, F. Borzumati, A. Masiero, G. Ridolfi, *Nucl. Phys.* **B353**, 591 (1991).

[2] G. Degrassi, P. Gambino, G.F. Giudice, *J. High Energy Phys.* **0012**, 009 (2000).

[3] M. Carena, D. Garcia, U. Nierste, C.E. Wagner, *Phys. Lett.* **B499**, 141 (2001).

[4] P. Cho, M. Misiak, *Phys. Rev.* **D49**, 5894 (1994).

[5] K. Fujikawa, A. Yamada, *Phys. Rev.* **D49**, 5890 (1994).

[6] C. Bobeth, M. Misiak, J. Urban, *Nucl. Phys.* **B567**, 153 (2000).

[7] F. Blanc, talk presented at the *XXXVIth Rencontres de Moriond*, Les Arcs, March 2001.

[8] G. Taylor, talk presented at the *XXXVIth Rencontres de Moriond*, Les Arcs, March 2001.

[9] R. Barate *et al.*, *Phys. Lett.* **B429**, 169 (1998).

[10] R. Balest *et al.*, *Phys. Rev.* **D52**, 2661 (1995).

[11] D.L. Scharre *et al.*, *Phys. Rev.* **D23**, 43 (1981).

[12] J. Chay, H. Georgi, B. Grinstein, *Phys. Lett.* **B247**, 399 (1990).

[13] A.L. Kagan, M. Neubert, *Eur. Phys. J.* **C7**, 5 (1999).

[14] C. Bauer, M. Luke, T. Mannel, `hep-ph/0102089`.

[15] T. Inami, C.S. Lim, *Prog. Theor. Phys.* **65**, 297 (1981); *Prog. Theor. Phys.* **65**, 1772 (1981) (E).

[16] S. Bertolini, F. Borzumati, A. Masiero, *Phys. Rev. Lett.* **59**, 180 (1987).

[17] N.G. Deshpande, P. Lo, J. Trampetic, G. Eilam, P. Singer, *Phys. Rev. Lett.* **59**, 183 (1987).

[18] R. Grigjanis, P.J. O'Donnell, M. Sutherland, H. Navelet, *Phys. Lett.* **B213**, 355 (1988); *Phys. Lett.* **B286**, 413 (1992) (E).

[19] B. Grinstein, R. Springer, M.B. Wise, *Nucl. Phys.* **B339**, 269 (1990).

[20] G. Cella, G. Curci, G. Ricciardi, A. Viceré, *Phys. Lett.* **B248**, 181 (1990); *Phys. Lett.* **B325**, 227 (1994).

[21] M. Misiak, *Phys. Lett.* **B269**, 161 (1991); *Phys. Lett.* **B321**, 113 (1994); *Nucl. Phys.* **B393**, 23 (1993); *Nucl. Phys.* **B439**, 461 (1995) (E).

[22] K. Adel, Y.P. Yao, *Mod. Phys. Lett.* **A8**, 1679 (1993).

[23] M. Ciuchini, E. Franco, G. Martinelli, L. Reina, L. Silvestrini, *Phys. Lett.* **B316**, 127 (1993).

[24] M. Ciuchini, E. Franco, L. Reina, L. Silvestrini, *Nucl. Phys.* **B421**, 41 (1994).

[25] A.J. Buras, M. Misiak, M. Münz, S. Pokorski, *Nucl. Phys.* **B424**, 374 (1994).

[26] M. Misiak, M. Münz, *Phys. Lett.* **B344**, 308 (1995).

[27] K. Chetyrkin, M. Misiak, M. Münz, *Phys. Lett.* **B400**, 206 (1997); *Phys. Lett.* **B425**, 414 (1998) (E); *Nucl. Phys.* **B518**, 473 (1998).

[28] C. Greub, T. Hurth, D. Wyler, *Phys. Rev.* **D54**, 3350 (1996).

[29] K. Adel, Y.P. Yao, *Phys. Rev.* **D49**, 4945 (1994).

[30] C. Greub, T. Hurth, *Phys. Rev.* **D56**, 2934 (1997).

[31] A.J. Buras, A. Kwiatkowski, N. Pott, *Nucl. Phys.* **B517**, 353 (1998).

[32] M. Ciuchini, G. Degrassi, P. Gambino, G.F. Giudice, *Nucl. Phys.* **B527**, 21 (1998).

[33] C. Bobeth, M. Misiak, J. Urban, *Nucl. Phys.* **B574**, 291 (2000).

[34] A. Ali, C. Greub, *Phys. Lett.* **B361**, 146 (1995).

[35] N. Pott, *Phys. Rev.* **D54**, 938 (1996).

[36] A. Czarnecki, W. Marciano, *Phys. Rev. Lett.* **81**, 277 (1998).

[37] K. Baranowski, M. Misiak, *Phys. Lett.* **B483**, 410 (2000).

[38] P. Gambino, U. Haisch, *J. High Energy Phys.* **09**, 001 (2000).

[39] A.F. Falk, M. Luke, M.J. Savage, *Phys. Rev.* **D49**, 3367 (1994).

[40] M.B. Voloshin, *Phys. Lett.* **B397**, 275 (1997).

[41] A. Khodjamirian, R. Rückl, G. Stoll, D. Wyler, *Phys. Lett.* **B402**, 167 (1997).

[42] Z. Ligeti, L. Randall, M.B. Wise, *Phys. Lett.* **B402**, 178 (1997).

[43] A.K. Grant, A.G. Morgan, S. Nussinov, R.D. Peccei, *Phys. Rev.* **D56**, 3151 (1997).

[44] G. Buchalla, G. Isidori, S.J. Rey, *Nucl. Phys.* **B511**, 594 (1998).

[45] A.J. Buras, A. Kwiatkowski, N. Pott, *Phys. Lett.* **B414**, 157 (1997); *Phys. Lett.* **B434**, 459 (1998) (E).

[46] P. Gambino, M. Misiak, `hep-ph/0104034`.

[47] A.H. Hoang, Z. Ligeti, A.V. Manohar, *Phys. Rev. Lett.* **82**, 277 (1999); *Phys. Rev.* **D59**, 074017 (1999).

[48] A.H. Hoang, `hep-ph/0008102`.